UDC 532.526:534.1

SPACE-TIME CHARACTERISTICS OF WALL PRESSURE FLUCTUATIONS ON THE SURFACE OF FLEXIBLE EXTENDED CYLINDER

V. A. Voskoboinick†, V. T. Grinchenko, O. A. Voskoboinyk, A. V. Voskobiinyk

Institute of Hydromechanics of NAS of Ukraine
8/4, Marii Kapnist Str., 03057, Kyiv, Ukraine
†*E-mail: vlad.vsk@gmail.com*

Received 24.10.2024

Generation of the hydrodynamic or aerodynamic noise is a well-known problem for vehicles and structures moving in water or air media. Therefore, predicting and controlling the properties of the turbulent hydrodynamic pseudoacoustic sources is of great importance. This paper presents the results of an experimental study of the cross-correlations and cross-spectra of wall pressure fluctuations on the surface of a longitudinally streamlined flexible cylinder. The degree of conversion of flow energy into the energy of the wall pressure fluctuation field is shown to be limited by a certain threshold. Its value corresponds to the ratio of the root-mean-square wall pressure fluctuation to the dynamic pressure of the order of 0.01 on a hydraulically smooth streamlined surface under a turbulent boundary layer with zero pressure gradient. The space-time correlation of wall pressure fluctuations along the generatrix of a flexible extended cylinder decreases with increasing distance between observation points, and the maximum values of the cross-correlation are observed for longer delay times. Convection of coherent vortex structures over the streamlined cylinder surface leads to an increase in the coherence levels of the wall pressure fluctuation field. Moreover, changes in the phase spectrum presented by sloping curves are observed. Their slope decreases with increasing convective velocity. The rate of degeneration of the maximum values of the space-time correlation coefficient in a wide frequency range on a flexible cylinder is higher than on a plate. Small-scale vortices that generate high-frequency pressure oscillations degenerate faster and are transported more slowly than large-scale coherent vortical structures from the outer region of the boundary layer. The obtained results are useful for the designers of the towed linear receiving hydroacoustic arrays.

KEY WORDS: space-time characteristics, wall pressure fluctuation, flexible cylinder, cross-correlation, coherence, phase spectrum

DOI: https://doi.org/10.15407/jha2024.04.412

1. INTRODUCTION

Generation of the hydrodynamic or aerodynamic noise is a big problem for many vehicles and structures that move in water or air. Hydrodynamic noise interferes with the operation of hydroacoustic systems in the fishing industry, the marine seismic antennas for minerals at the bottom of seas and oceans, the operation of hydroacoustic stations and antennas on surface and underwater ships [1–5]. When flexible extended cylinders or other objects move in water, turbulent boundary layers form above their surfaces, which generate velocity and pressure fluctuations. Wall pressure fluctuations, which have a sonic and pseudosonic (aerohydrodynamic) nature, are sources of noise from shear turbulent flows [6–9]. Hydrodynamic noise disrupts the operation of hydroacoustic sensors, which are located under the elastic cylindrical shell of the cylinder. The sound generated by the boundary layer has a wave nature and propagates into the environment at the speed of sound, while pseudosonic pressure oscillations propagate at a velocity close to the flow velocity. Large-scale and small-scale vortex structures of the boundary layer are sources of pseudosound. These vortex structures form the outer and inner regions of the boundary layer, have different lifetimes and convective velocities, and interact nonlinearly with each other and with the streamlined surface [10, 11]. Pseudosound does not obey the superposition principle, does not propagate beyond the boundary layer, and pseudosound pressure does not depend on the average pressure of the medium and decreases inversely with the square of the distance from the source [3, 6, 12–15].

Wall pressure fluctuations integrally reflect the presence of velocity fluctuations in the boundary layer [3, 16–18]. The nature and intensity of the field of pressure fluctuations on the streamlined surface are largely determined by the motion of coherent vortex structures. The study of the physics of turbulent pressure fluctuations is important not only because they are sources of hydrodynamic noise, but also because they excite the streamlined surface and induce vibrations. In addition, turbulent pressure fluctuations are present in correlation dependences in the transfer equations for Reynolds stresses and the energy dissipation tensor.

Simulation of the pressure fluctuation field is carried out using numerical models based on the solution of the Poisson equation, as well as semi-empirical models. The complexity of solving the Poisson equation lies in the fact that the velocity fluctuations of all parts of the boundary layer contribute to the wall pressure fluctuation field [19–22]. The sources of turbulent velocity and pressure fluctuations have different scales, are located in different regions of the boundary layer, and have different convective velocities. Studies [23–25] have shown that there are large-scale motions in a turbulent boundary layer and very-large-scale motions in the outer region of the boundary layer, which have a significant effect on near-wall turbulence. These motions and vortex structures interact with small-scale near-wall vortices, modulate their motion, decrease or increase their intensity [26–29]. This makes it difficult to find acceptable scaling laws for external, internal, or mixed variables in order to describe the velocity and pressure fields in the boundary layer [30, 31]. Thus, the low-frequency components of the spectrum of pressure fluctuations, which are due to the action of large-scale vortex structures, are scaled by external variables of the boundary layer. Small-scale near-wall vortices generate high-frequency fluctuations and are scaled by internal variables [32,33].

The Poisson equation for an incompressible fluid confirms that pressure fluctuations are generated by two mechanisms, namely, by the interaction of velocity fluctuations with av-

eraged velocity gradients and by the interaction of turbulence with turbulence. Turbulent flows are volumetric, vortex, irregular, and unstable, and represent motions with a random change of flow properties in time and space. Due to unevenness and randomness, it is impossible to describe in detail the motion of a fluid as a function of time and spatial coordinates. Therefore, the laws of probability theory and mathematical statistics are used to describe turbulent flows [16, 34–37].

The experimental database is the basis for constructing integral, correlation, and spectral dependences in semi-empirical models. For example, in the works [19,38,39], integral models of the pressure fluctuation field were proposed. Spectral models of pressure fluctuations in frequency and wave domains were proposed in the works [40–47]. Detailed comparisons of pressure fluctuation field models and wall pressure fluctuation sources are presented in [16, 35, 48–50]. The spectral ranges are divided into the low frequency region, which, according to the Kraichnan-Phillips theorem, is proportional to the square of the frequency [38,51,52]. The mid-frequency region, which corresponds to the inertial range, is varied inversely with frequency, as indicated in [43, 53, 54]. The high-frequency part of the pressure fluctuation spectrum is proportional to frequency to the power of -5 [39, 55–57].

The goal of this study is to determine the space-time characteristics of wall pressure fluctuations on the surface of a flexible longitudinally streamlined extended cylinder, as well as to study the generation and evolution of the sources of these fluctuations.

2. EXPERIMENTAL SETUP AND RESEARCH PROGRAM

The experiments were conducted in a hydrodynamic channel with the following dimensions: about 4000 m long, 40 m wide, and about 5 m deep. The channel was characterized by minimal flow and the absence of navigation; the banks were covered by vegetation. The noise in the channel was below the lower boundary of the prevailing noise of the sea, which ensured the conduct of high-quality hydroacoustic research. A cylinder in the form of a flexible extended cylinder with a length (L) of up to 20 m and a diameter (D) from $16 \cdot 10^{-3}$ m to $44 \cdot 10^{-3}$ m was towed at a depth of 1.2 m. The cylinder was fixed with the help of a streamlined knife at the aft of a streamlined and low-noise catamaran (Fig. 1). The stabilizing devices and the cylinder tension device were installed at the aft of the extended cylinder. The boat towed the well-streamlined catamaran at a distance of about 160 m (to reduce the noise of the boat). Towing velocity (U) varied from 3 m/s to 6 m/s.

The flexible extended cylinder (Fig. 1) consisted of three cylindrical sections (damping, idle, and measurement ones), in which the sensors (measurement section), shielded electrical conductors, centering rings, and sealed electrical connectors were located. A nylon cord was used as the power element in the damping section (to reduce structural interference), and in the measurement and idle section, the power element was a steel cable. The idle and measurement sections could be replaced by places to study the sources of hydrodynamic noise along the cylinder length and to increase the Reynolds number.

Miniature piezoceramic wall pressure fluctuations sensors, hydrophones, and accelerometers were installed inside the measurement section (Fig. 2). The accelerometers (position *S1*) measured the cylinder vibrations in three mutually perpendicular planes, while pressure fluctuation sensors (position *S2*) and hydrophones (position *S3*) measured hydroacoustic parameters. The pressure fluctuation sensors were installed flush with the streamlined cylinder

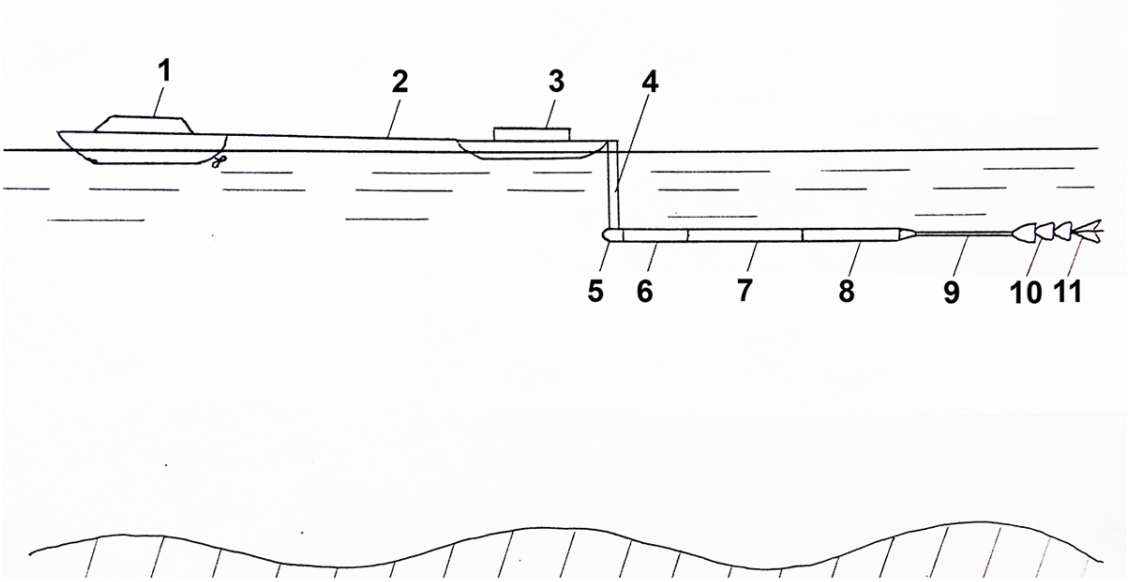

Fig. 1. Towing scheme:
1 — boat, *2* — capron cord, *3* — catamaran, *4* — knife, *5* — bow, *6* — damping section, *7* — idle section, *8* — measurement section, *9* — extender, *10* — cylinder tension device, *11* — stabilizing device

surface and did not disturb the flow. Hydrophones and accelerometers were installed under the elastic cylinder sheath of the measurement section. The sensitive surface area of the hydrophones was more than a thousand times larger than that of pressure fluctuation sensors, so they recorded only the low-frequency part of the hydrodynamic noise spectrum. Pressure fluctuation sensors were located both individually (position *S2* and in correlation blocks (positions *S6–S9* and *S10–S12*) to record the cross-spectra and correlation characteristics of the wall pressure fluctuation field.

Miniature piezoceramic sensors of the membrane type were specially designed and manufactured for research. Wall pressure fluctuation sensors (Fig. 3) had a sensitive surface diameter (d) of $1.3 \cdot 10^{-3}$ m and $1.6 \cdot 10^{-3}$ m. They had a high spatial resolution and operation velocity [34, 55, 56, 58].

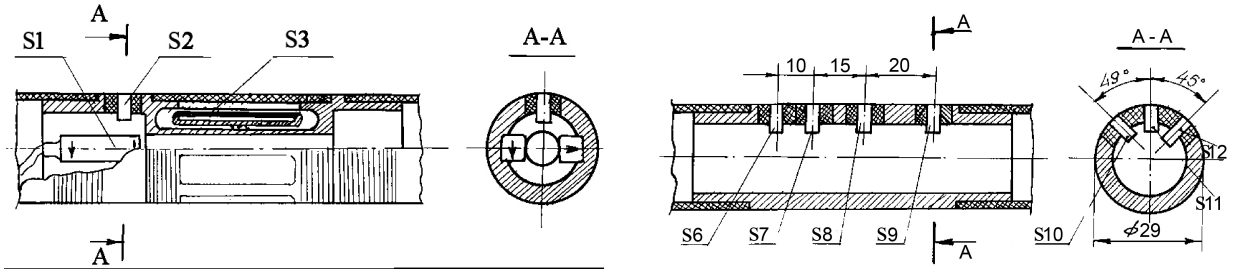

Fig. 2. Measuring instruments:
S1 — accelerometer, *S2* — pressure fluctuation sensor, *S3* — hydrophone, *S6–S12* — group of pressure fluctuation sensors nos. 6—12

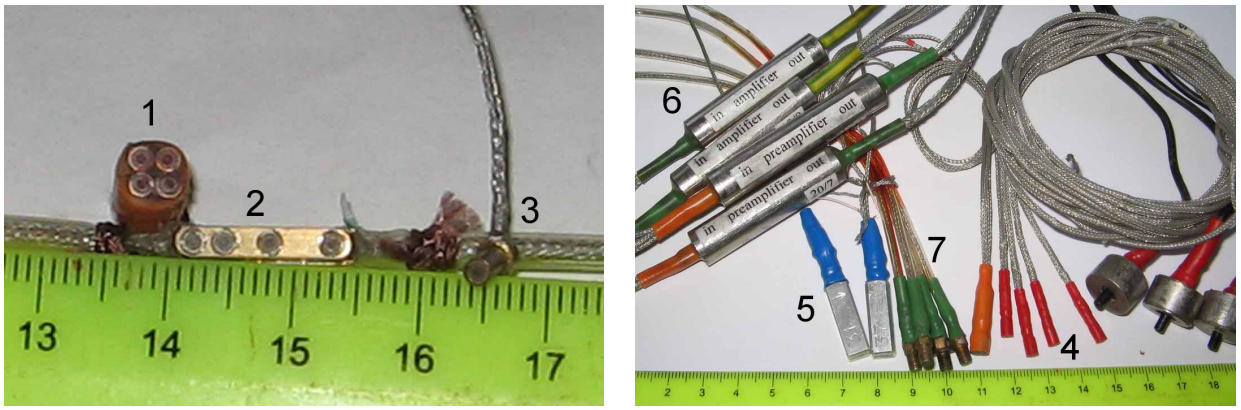

Fig. 3. Measuring and amplifying devices:
1, *2* — two types of the correlation blocks of pressure fluctuation sensors, *3* — single sensor, *4* — wall pressure fluctuation sensors, *5* — accelerometers, *6* — preamplifiers, *7* — pressure sensors

The pressure fluctuation sensors were equipped with preamplifiers (position *3* in Fig. 3b), which were located at minimum distances from the sensors in order to reduce electromagnetic interference. Electrical signals from preamplifiers through shielded communication lines are fed to low-noise power amplifiers connected to the control and measuring equipment. Data were recorded with four-channel measuring tape recorders 'Bruel & Kjær' (Denmark). Simultaneously with the measurements of pressure fluctuations, the vibrational situation of the cylinder was monitored using three-component miniature piezoceramic accelerometers (position *2* in Fig. 3b). The measurement results of the cylinder vibrations were used to compensate for the measurement results by appropriate methods. Data processing and analysis were carried out on one and two-channel spectrum analyzers 'Bruel & Kjær' using the fast Fourier transform algorithm. The analog signals of the vibration and pressure sensors were digitized using multichannel analog-to-digital converters and fed to personal computers. The digitized signals on computers were processed and analyzed using programs and methods of probability theory and mathematical statistics [37, 59, 60].

The pressure fluctuation sensors were calibrated by the absolute method on a specially made benchmark [61], where the specified pressure difference was pulsed. In addition, the sensors were calibrated using a specially developed technique in a reservoir where gravity waves were generated at a fixed height and oscillation period. The pressure fluctuation sensors were calibrated in Bruel & Kjær pistonphone type 4228 at fixed amplitudes and frequencies of oscillations. The sensors were calibrated using relative methods against reference microphones and hydrophones in near and far acoustic fields produced by harmonic emitters, as well as white and pink noise emitters. To control the sensitivity of pressure fluctuation sensors, relative measurements were performed periodically during experimental studies.

All pressure fluctuation sensors were tested on vibration benchmarks for calibrating Bruel & Kjær accelerometers type 4808 for the determination of the vibration sensitivity in three mutually perpendicular planes [55, 62, 63]. These characteristics were taken into account during vibration compensation of the measurement results. As a result, it was possible to achieve acceptable experimental conditions with a fairly high degree of accuracy and repeatability of the results. Integral characteristics of the pressure fluctuation field were obtained

with an error of no more than 5%. The measurement error of the spectral dependences did not exceed 2 dB in the frequency range from 0.2 Hz to 1.25 kHz, and the correlation characteristics were measured with an error of not more than 12% with a confidence probability of 0.95.

The field of wall pressure fluctuations on the streamlined surface of an extended flexible cylinder was recorded under turbulent flow conditions. For this flow regime, the Reynolds numbers, which were calculated from the towing velocity (U), the cylinder length to the sensor location (X), and the cylinder radius (R), were $\mathrm{Re}_X = UX/\nu = (15 \dots 120) \cdot 10^6$ and $\mathrm{Re}_R = UR/\nu = (2 \dots 13) \cdot 10^4$, where ν is the kinematic coefficient of viscosity. The boundary layer thickness (δ) over the streamlined surface of the cylinder varied from $2 \cdot 10^{-2}$ m to $5 \cdot 10^{-2}$ m, and the displacement thickness (δ^*) varied from $3 \cdot 10^{-3}$ m to $8 \cdot 10^{-3}$ m. Dynamic velocity varied (u_τ) from 0.11 m/s to 0.17 m/s. Thus, the flow around the flexible long cylinder with an elongation (L/D) from 110 to 1250, with a transverse curvature (δ/R) from 1.5 to 3.8 was studied.

3. RESULTS AND DISCUSSION

It is known that an increase in the sensitive surface of the wall pressure fluctuation sensor leads to a decrease in the recorded levels of pressure fluctuation spectra in the high-frequency region [16, 32, 35, 39]. This is due to the integrating effect concerning small-scale vortex structures that are formed in the wall region of the boundary layer. If the wavelength of sources of the wall pressure fluctuations is less than two sensor diameters, then the sensor is not able to distinguish them, and it works as a spatial filter. Such a sensor damps high-frequency fluctuations that are generated by small-scale vortices.

The ratio of the root-mean-square values of the wall pressure fluctuations to the velocity head or dynamic pressure ($q = \rho U^2/2$, where ρ is density of water), depending on the dimensionless diameter of the sensor ($d^+ = u_\tau d/\nu$), is shown in Fig. 4. Here the results of measurements in turbulent internal and external flows with a zero pressure gradient were presented, which were carried out both recessed under the hole and installed flush with the streamlined surface of the sensors or microphones. Markers indicate the results of experimental studies. The results marked with the indices *5*, *12*, *13*, and *15* were obtained in the research with sensors located under the holes on the streamlined surface.

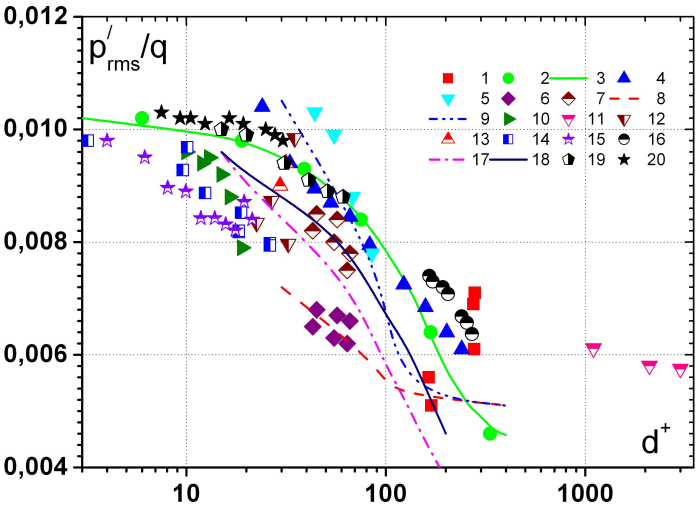

Fig. 4. Dependence of the acoustic-hydrodynamic coefficient on the diameter of the pressure fluctuation sensor, according to various sources:
1 — [64]; *2, 3* — [65]; *4* — [66]; *5* — [67]; *6–9* — [68]; *10* — [69]; *11* — [70]; *12* — [71]; *13* — [72]; *14* — [73]; *15* — [74]; *16* — [62]; *17–18* — [75]; *19* — [55]; *20* — [55]

As noted in papers [65, 74–76], an increase in the diameter of the sensitive surface of the sensor by more than 20 viscous wall units leads to a significant damping of the high-frequency spectral characteristics. In the paper [73], it was noted that the maximum permissible dimensionless diameter of the sensitive surface, which does not damp the spectral dependences up to the frequency $f\nu/u_t au^2 < 1$, is a diameter of $12 \leq d^+ \leq 18$. This requirement forces the design of highly sensitive and low-noise miniature sensors, which should be installed on a streamlined surface without violating its integrity [77]. Based on these requirements, miniature highly sensitive pressure fluctuation sensors were developed and manufactured [34, 55, 62], which had a diameter of the sensitive surface $d^+ \geq 7$.

The results of Fig. 4 show that with a decrease in the diameter of the sensitive surface of the wall pressure fluctuation sensor or the hole under the recessed microphones, the normalized rms values of the pressure fluctuations asymptotically tend to a certain limiting value. It was indicated in [65] that a point sensor ($d^+ \to 0$), which can measure all scales of the vortex structures of the boundary layer, can detect wall pressure fluctuations of intensity $\sqrt{\overline{(p')^2}}/q \approx 0.0102$. Consequently, on a hydraulically smooth streamlined surface (the roughness height does not exceed the thickness of a viscous sublayer) beneath a turbulent boundary layer with a zero pressure gradient, the transformation of the flow energy into the energy of the wall pressure fluctuation field has a limiting value, which corresponds to an acoustic-hydrodynamic coefficient of the order of 0.01. This applies to pressure fluctuation sensors, which have high sensitivity, performance, noise immunity, and a diameter of the sensitive surface of not more than 20 viscous wall units. Larger sensors measure the understated intensity of pressure fluctuations and do not record the high-frequency components of the spectrum, and therefore require corrective actions. Therefore, in aero- and hydroacoustic research, correction dependences are widely used, which are applied to the high-frequency region of the pressure fluctuation spectrum and integral characteristics of the pressure field (for example, correction factors and functions proposed in [16, 35, 40]).

Using a group of miniature pressure fluctuation sensors, it was possible to determine the space-time characteristics of the pressure fluctuation field on the streamlined surface of the cylinder and to reveal the features of the sources of these fluctuations [16, 17, 35, 55, 62, 78]. The most frequent objects of theoretical and experimental study are correlation moments or correlation functions [16, 36, 37, 39, 76]. The space-time correlation of two random variables, which are obtained for non-coincident space-time points ($\vec{x}_A \neq \vec{x}_B$; $t_1 \neq t_2$; $\vec{x}_A - \vec{x}_B = \vec{\xi}$; $t_1 - t_2 = \tau$), is characterized by a single non-random parameter [37]

$$R_p(\vec{\xi}, \tau) = \overline{p(\vec{x}_A, t_1)p(\vec{x}_B, t_2)} = \frac{1}{T}\int_0^T p(\vec{x}_A, t)p(\vec{x}_B, t+\tau)dt. \tag{1}$$

However, correlation, as a measure of statistical connection, has one significant disadvantage: it depends on the amplitudes of the quantities that are measured. The correlation coefficient, which is a correlation moment normalized by the product of the standard deviations of random variables, is devoid of this disadvantage. The cross or space-time correlation coefficient is defined as

$$\rho_p(\vec{\xi}, \tau) = \frac{\overline{p(\vec{x}_A, t_1)p(\vec{x}_B, t_2)}}{\sigma(\vec{x}_A, t_1)\sigma(\vec{x}_B, t_2)}, \tag{2}$$

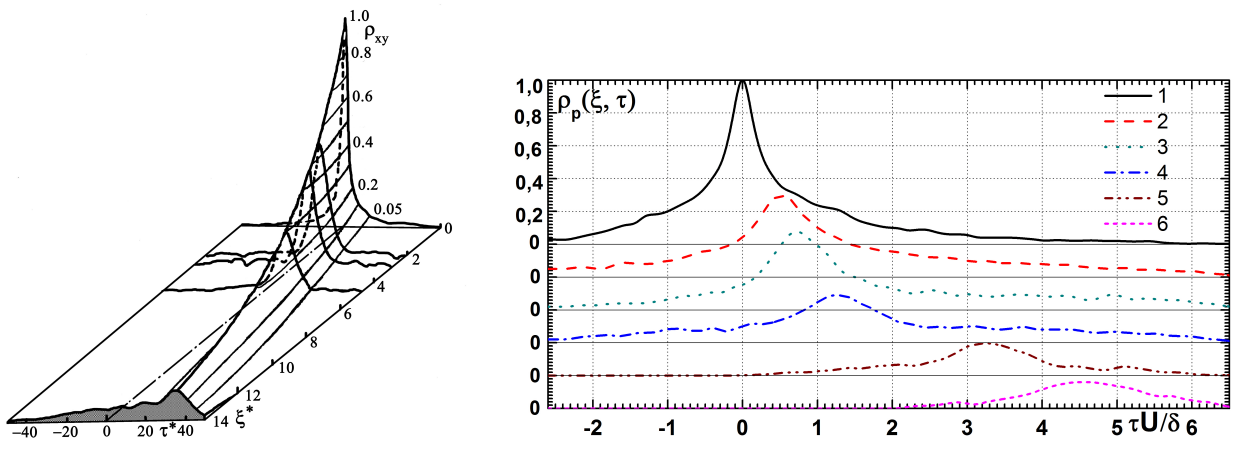

a *b*

Fig. 5. Space-time correlation coefficients of the wall pressure fluctuations:
a — the dependence on the separation between sensors and the delay time; *b* — for different delay times;
1 — $\xi/\delta = 0$, *2* — $\xi/\delta = 0.29$, *3* — $\xi/\delta = 0.44$, *4* — $\xi/\delta = 1.32$, *5* — $\xi/\delta = 2.79$, *6* — $\xi/\delta = 4.12$

where $\sigma(\vec{x}_A, t_1)$ and $\sigma(\vec{x}_B, t_2)$ are the root mean square values of pressure fluctuations in points A and B.

In the particular case of coinciding reference moments and non-coincident observation points ($t_1 = t_2$; $\vec{x}_A \neq \vec{x}_B$), we will have a spatial correlation. In another particular case, when the observation points coincide, but the reference times differ ($\vec{x}_A = \vec{x}_B$; $t_1 \neq t_2$), we will have an autocorrelation function.

Fig. 5 shows the coefficients of space-time or cross correlations of the wall pressure fluctuations, which were measured along the generatrix of the streamlined flexible cylinder and calculated from dependence (3). The cylinder had a transverse curvature of 3.2 and it was streamlined by a turbulent flow, for which the Reynolds numbers were $\mathrm{Re}_X \approx 4 \cdot 10^7$ and $\mathrm{Re}_R \approx 7 \cdot 10^4$. The measurements of the field of the wall pressure fluctuations were carried out by a group of sensors that were at different separations from each other (ξ).The separation between the sensors and the delay time in Fig. 5a are normalized by external variables, namely, the towing velocity and the displacement thickness of the boundary layer ($\xi^* = \xi/\delta^*$ and $\tau^* = \tau U/\delta^*$). The towing velocity and the thickness of the boundary layer normalized the delay time on Fig. 5b. The results of the study showed that with an increase in the separation between the sensors, the correlation of the wall pressure fluctuations along the generatrix of the cylinder decreases. Moreover, the maxima of the cross-correlation coefficient were observed at a longer delay time (τ).

The attenuation of the maximum values of the space-time correlation coefficients of wall pressure fluctuations along the flat plate and the generatrix of the cylinder for different separations between wall pressure sensors and the delay time is shown in Figs. 6 and 7. In Fig. 6, curve *1* was obtained in [79] on a flat plate in the frequency range $0.46 \leq f\delta/U \leq 7.55$, curve *2* was measured on a flexible extended cylinder with curvature $\delta/R = 3$ in the frequency range $0.30 \leq f\delta/U \leq 6.34$ and curve *3* was obtained in [80] on a rigid extended cylinder

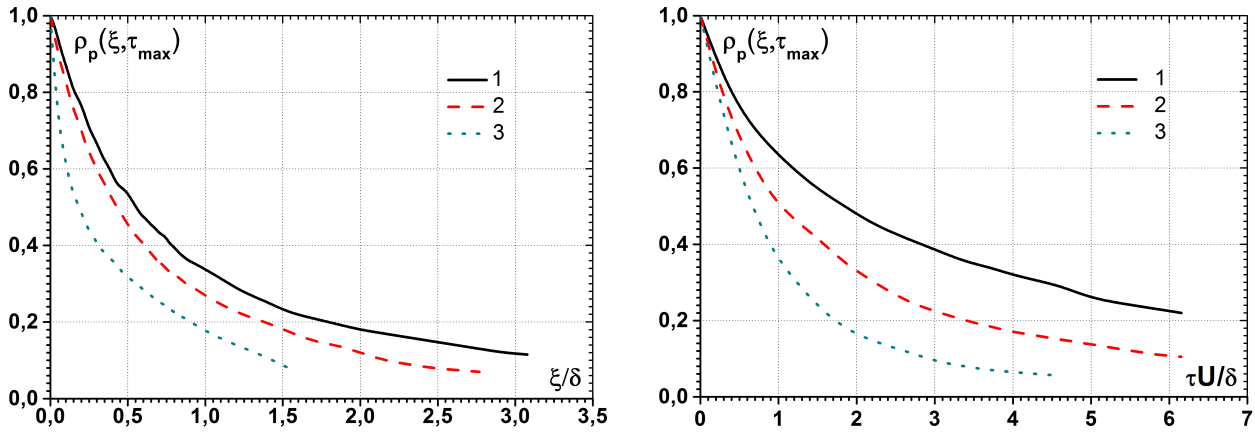

Fig. 6. Maxima of the space-time correlation coefficients on the flat plate and the cylinder: *1* — $\delta/R = 0$ and $0.46 \le f\delta/U \le 7.55$ plate [79]; *2* — $\delta/R = 3$ and $0.30 \le f\delta/U \le 6.34$, flexible cylinder; *3* — $\delta/R = 2$ and $0.15 \le f\delta/U \le 30$, rigid cylinder [80]

Fig. 7. Maxima of the space-time correlation coefficients on the flexible cylinder in the different frequency ranges: *1* — $0.15 \le f\delta/U \le 0.48$, *2* — $0.15 \le f\delta/U \le 3.12$, *3* — $0.30 \le f\delta/U \le 6.34$

with curvature $\delta/R = 2$ in the frequency range $0.15 \le f\delta/U \le 30$. It was found that on the flexible cylinder, the attenuation rate of the maximum values of the cross-correlation coefficients was higher than on the plate but lower than on the rigid cylinder. In Fig. 7, curve *1* was obtained for a flexible cylinder in the frequency range $0.15 \le f\delta/U \le 0.48$, curve *2* corresponds to the frequency range $0.15 \le f\delta/U \le 3.12$, and curve *3* – to the frequency range $0.30 \le f\delta/U \le 6.34$. The lifetime of pressure forming large-scale vortex structures generating the low-frequency wall pressure fluctuations, was 4 to 5 times higher than that of small-scale low-velocity vortices that generated high-frequency fluctuations of the pressure field on the cylindrical surface.

The lines of equal values of the cross-correlation coefficients in the plane ξ and τ, which were also normalized by the external variables of the boundary layer, are shown in Fig. 8. The measurements were carried out on the extended cylinder, which had the transverse curvature $\delta/R \approx 2.5$. The results in Fig. 8a were obtained for the Reynolds numbers of $\mathrm{Re}_X = 4 \cdot 10^7$ and $\mathrm{Re}_R = 7 \cdot 10^4$. The results in Fig. 8b were obtained for Reynolds numbers of $\mathrm{Re}_X = 7 \cdot 10^7$ and $\mathrm{Re}_R = 1 \cdot 10^5$. Here, curve *1* displays the values of the space-time correlation coefficients of the wall pressure fluctuations, which were measured along the generatrix of the cylinder. Curve *2* corresponds to the maximum cross-correlation coefficient for the corresponding ξ and τ. It was found that with an increase in the separation between the sensors and the delay time, a larger slope of the cross-correlation maximum curves was observed. In addition, the values of the cross-correlation coefficient with growth ξ decrease, as illustrated in Fig. 5, and the shape of the curves becomes gentler.

The ratio of separation between the sensors and the delay time allowed determining the longitudinal convective velocity of the coherent vortex structures [16, 62]. A group transfer velocity was determined in the form, and a local convective velocity was determined in the form $u_{cg} = \Delta\xi/\Delta\tau_{\max}$ (see Fig. 8). The longitudinal convective velocities of the coherent

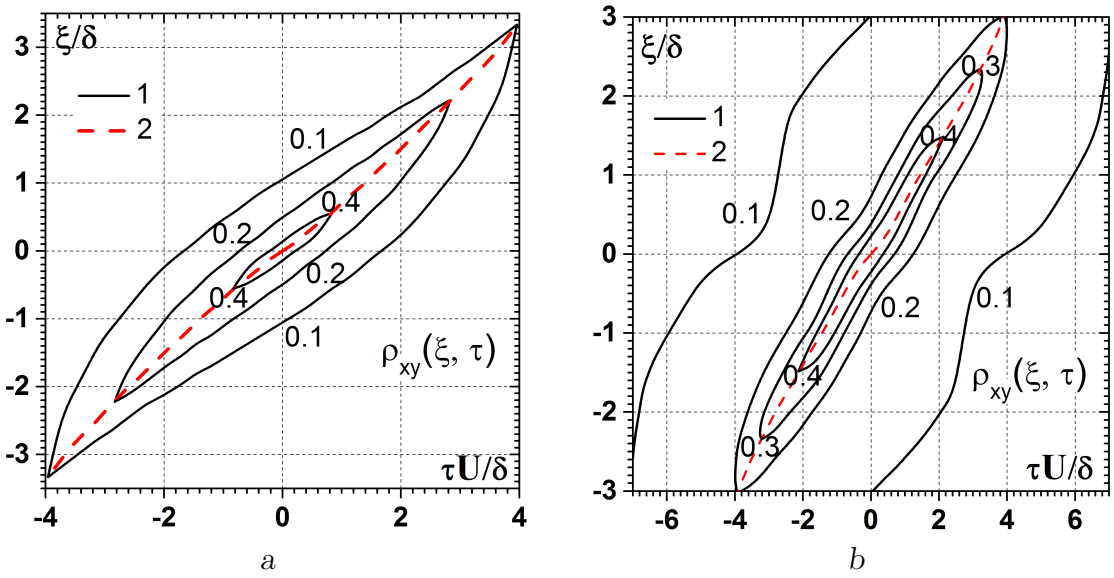

Fig. 8. The lines of equal values of the cross-correlation coefficients:
a — for $\mathrm{Re}_X = 4 \cdot 10^7$ and $\mathrm{Re}_R = 7 \cdot 10^4$, *b* — for $\mathrm{Re}_X = 7 \cdot 10^7$ and $\mathrm{Re}_R = 1 \cdot 10^5$;
1 — space-time correlation coefficients, *2* — the maximum cross-correlation coefficient

vortex structures are shown in Figs. 9 and 10. Therefore, the group velocity of the transfer of vortex structures with increasing separation between the sensors increased. Since the sources of velocity and pressure fluctuations in turbulent boundary layers are vortex structures, large-scale vortices that are located in the outer region of the boundary layer remain correlated for large separations [17, 32, 62]. Their convective velocity is higher than the velocity of small-scale near-wall vortices, which follows from the results of measurements of space-time correlations, which are presented in Fig. 5. In addition, the values of the cross-correlation coefficients with growth ξ decrease, and the shape of the curves becomes gentler.

Fig. 9 shows the group convective velocity, and curve *1* was obtained from studies on the flexible extended cylinder of the transverse curvature $\delta/R \approx 2.5$ and Reynolds numbers and $\mathrm{Re}_R = 7 \cdot 10^4$. Curve *2* was measured in research of the wall pressure fluctuations on the hydraulically smooth plate in the study [79], curves *3* and *4* were obtained in studies [80] and [78] for investigations on the cylinders of the transverse curvature $\delta/R = 2$ and $\delta/R = 4$. Curve *5* was measured on the smooth plate in research [64], curves *6* and *7* were obtained in research [67] for the smooth and rough plate ($k^+ = ku_\tau/\nu = 186.8$, where k is the roughness height), respectively. The research results show that the group convective velocity of coherent vortex structures, which were generated above the surface of the flexible cylinder, was higher than above the surface of the rigid cylinder and above the surface of the smooth and rough plate. Along with this, it should be noted that with an increase in the separation between the wall pressure fluctuation sensors, the longitudinal convective velocity of the coherent vortex structures increases. This is since, as noted earlier, the large-scale vortex structures that form the outer region of the boundary layer remain correlated at large separations between the sensors and the small-scale vortices of the inner region of the boundary layer degenerate.

Fig. 10 presents the results of measurements of the local convective velocity of the coherent vortex structures of the boundary layer, which generate correlated wall pressure fluc-

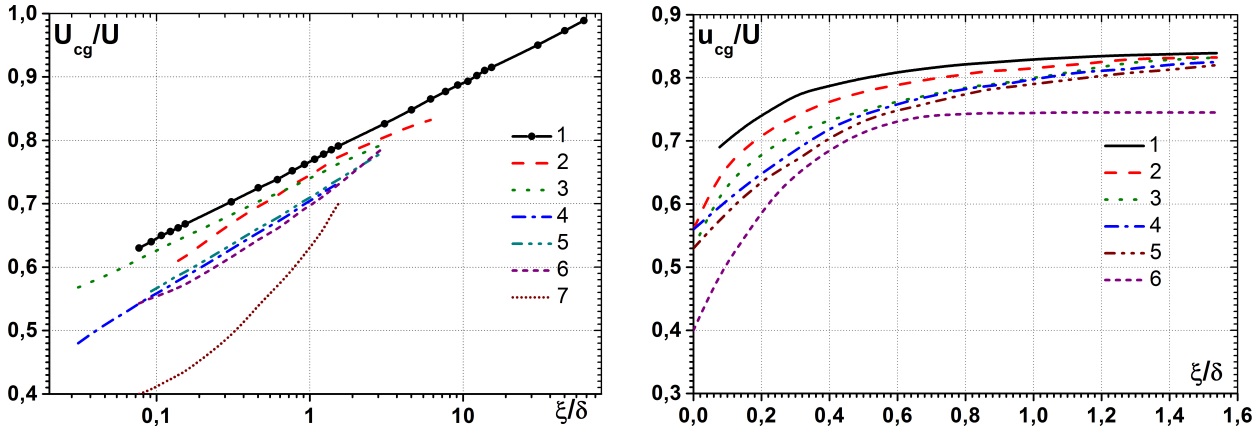

Fig. 9. The longitudinal convective group transfer velocity of the coherent vortex structures: *1* — $\delta/R \approx 2.5$, $\mathrm{Re}_X = 4 \cdot 10^7$ and $\mathrm{Re}_R = 7 \cdot 10^4$, flexible cylinder; *2* — hydraulically smooth plate [79]; *3* — $\delta/R = 2$, rigid cylinder [80]; *4* — $\delta/R = 4$, rigid cylinder [78]; *5* — smooth plate [64]; *6* — smooth plate [67]; *7* — rough plate, $k^+ \approx 187$ [67]

Fig. 10. The longitudinal local convective velocity of the coherent vortex structures: *1* — $\delta/R \approx 2.5$, $\mathrm{Re}_X = 4 \cdot 10^7$ and $\mathrm{Re}_R = 7 \cdot 10^4$, flexible cylinder; *2* — hydraulically smooth plate [79] and $\delta/R = 2$, rigid cylinder [80]; *3* — $\delta/R = 4$, rigid cylinder [78]; *4* — smooth plate [64]; *5* — smooth plate [67]; *6* — rough plate, $k^+ \approx 187$ [67]

tuations on the streamlined surface. Curve *1* was measured on the flexible cylinder with transverse curvature $\delta/R \approx 2.5$ and Reynolds numbers $\mathrm{Re}_X = 4 \cdot 10^7$ and $\mathrm{Re}_R = 7 \cdot 10^4$, curve *2* is the results of studies [79] and [80] for the smooth plate and rigid cylinder with the transverse curvature $\delta/R = 2$, curve *3* is the results of measurements on the smooth plate [64], curve *4* is the results of the study [78] for the rigid cylinder of the transverse curvature $\delta/R = 4$ and curves *5* and *6* were obtained in research [67] for the smooth and rough plate. The results showed that the local longitudinal convective velocities of the coherent vortex structures were also higher in the turbulent boundary layer above the flexible extended cylinder. This indicates that in the boundary layer above the flexible cylinder, the large-scale vortex structures were located further away from the streamlined surface, where the convective velocity was higher.

The cross power spectral density of the wall pressure fluctuations, or simply the cross-spectrum, is the Fourier transform of the space-time correlation (3) and is determined by the dependence [37]

$$S_p(\vec{\xi}, \omega) = \frac{1}{2\pi} \int_{-\infty}^{\infty} R_p(\vec{\xi}, \tau) e^{-j\omega\tau} d\tau \tag{3}$$

or

$$P(\vec{\xi}, \omega) = \frac{1}{\pi} \int_{0}^{\infty} R_p(\vec{\xi}, \tau) e^{-j\omega\tau} d\tau = C(\vec{\xi}, \omega) - jQ(\vec{\xi}, \omega), \tag{4}$$

where $C(\vec{\xi}, \omega)$ is the in-phase component of the cross-spectrum (in-phase spectrum), and $Q(\vec{\xi}, \omega)$ is the quadrature component of the cross-spectrum (quadrature spectrum). These

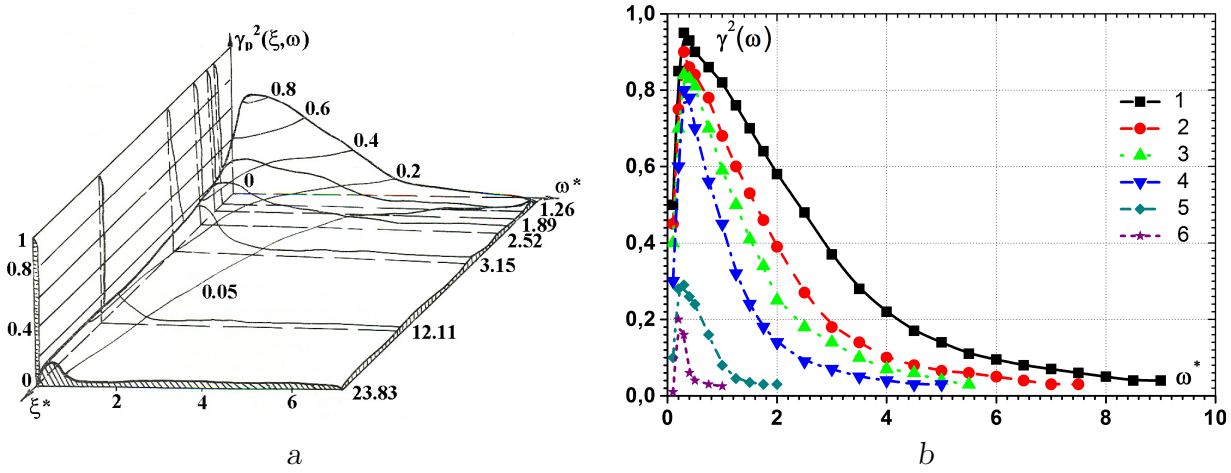

a *b*

Fig. 11. The coherence functions of the wall pressure fluctuations along the generatrix of the flexible extended cylinder:
a — three-dimensional plot, *b* — frequency dependence;
1 — $\xi/\delta = 0.19$, *2* — $\xi/\delta = 0.29$, *3* — ξ/δ=0.39,
4 — $\xi/\delta = 0.48$, *5* — $\xi/\delta = 1.86$, *6* — $\xi/\delta = 3.67$

components of the cross-spectrum are determined from the following expressions:

$$C(\vec{\xi},\omega) = \frac{1}{\pi}\int_0^\infty R_p(\vec{\xi},\tau) + R_p(-\vec{\xi},\tau)\cos(\omega\tau)d\tau, \tag{5}$$

and

$$Q(\vec{\xi},\omega) = \frac{1}{\pi}\int_0^\infty R_p(\vec{\xi},\tau) - R_p(-\vec{\xi},\tau)\sin(\omega\tau)d\tau. \tag{6}$$

Since the space-time correlation function does not have the parity property, the cross-spectral density is a complex function of frequency [37]. The cross-spectrum can be presented in an exponential form

$$P(\vec{\xi},\omega) = |P(\vec{\xi},\omega)|\exp[-j\Theta(\vec{\xi},\omega)]. \tag{7}$$

The absolute value of the cross-spectrum $|P(\vec{\xi},\omega)|$ and its phase $\Theta(\vec{\xi},\omega)$ can be expressed through the in-phase $C(\vec{\xi},\omega)$ and quadrature $Q(\vec{\xi},\omega)$ components of the cross-spectrum in the form

$$|P(\vec{\xi},\omega)| = \sqrt{C^2(\vec{\xi},\omega) + Q^2(\vec{\xi},\omega)} \tag{8}$$

and

$$\Theta(\vec{\xi},\omega) = \operatorname{arctg}\frac{Q(\vec{\xi},\omega)}{C(\vec{\xi},\omega)}. \tag{9}$$

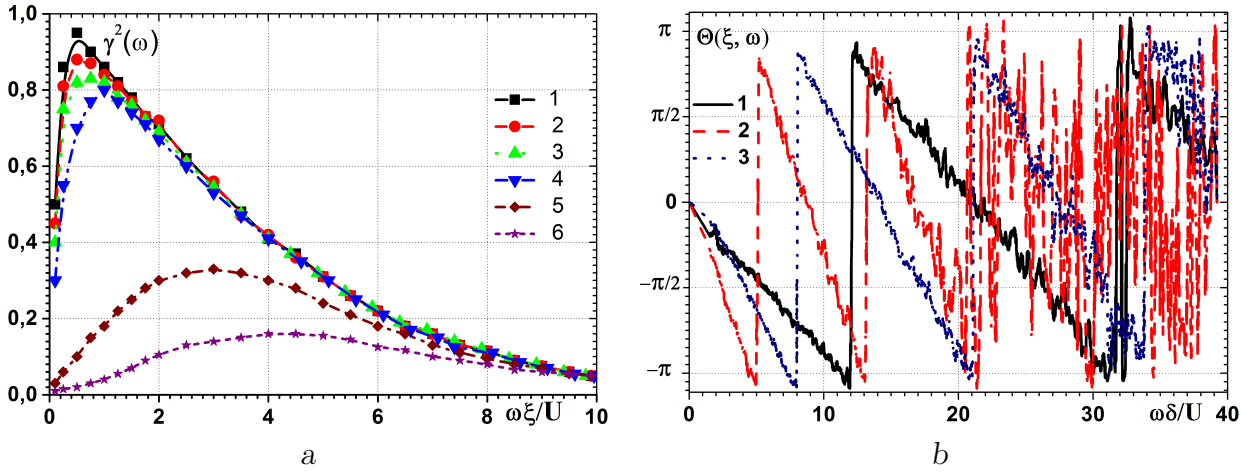

Fig. 12. Components of the cross-spectrum of the wall pressure fluctuations:
a — coherence functions, b — phase spectra;
1 — $\xi/\delta = 0.19$, 2 — $\xi/\delta = 0.29$, 3 — $\xi/\delta = 0.39$,
4 — $\xi/\delta = 0.48$, 5 — $\xi/\delta = 1.86$, 6 — $\xi/\delta = 3.67$;

To solve physical problems, the real part of the cross-spectral density is used, which is called the coherence function and is expressed as [16, 35, 37, 81]

$$\gamma^2(\vec{\xi}, \omega) = \frac{|P(\vec{\xi}, \omega)|^2}{P_A(0, \omega) P_B(0, \omega)} \leq 1. \tag{10}$$

The coherence functions of the wall pressure fluctuations, which were measured along the generatrix of the flexible extended cylinder and calculated from dependence (3), are presented in Fig. 11. The coherence functions were measured on the cylinder, which had the transverse curvature $\delta/R = 2$ and was towed at the velocity of $U = 5$ m/s. The Reynolds numbers for this flow regime were $\mathrm{Re}_X = 9 \cdot 10^7$ and $\mathrm{Re}_R = 7 \cdot 10^4$. Fig. 11a presents the coherence functions in dependence on the separation between the wall pressure fluctuation sensors and the frequency, which were normalized by the displacement thickness of the boundary layer δ^* and the towing velocity U.

The coherence functions (Fig. 11b) were measured for the following separations between the sensors: curve 1 – $\xi/\delta = 0.19$, curve 2 – $\xi/\delta = 0.29$, curve 3 – $\xi/\delta = 0.39$, curve 4 – $\xi/\delta = 0.48$, curve 5 – $\xi/\delta = 1.86$ and curve 6 – $\xi/\delta = 3.67$. The frequency was normalized by the displacement thickness of the boundary layer and the towing velocity as $\omega^* = \omega\delta^*/U$. So, with an increase in the separation between the sensors and the frequency, the coherence of the pressure fluctuation field decreased, since small-scale vortex structures lose their individuality faster than large-scale coherent vortex structures.

Cross-spectral dependences of the wall pressure fluctuation field in the form of coherence functions and phase spectra measured along the generatrix of the longitudinally streamlined cylinder are shown in Fig. 12. The coherence functions (Fig. 12a) were measured for the separations between the wall pressure fluctuation sensors: curve 1 – $\xi/\delta = 0.19$, curve 2 – $\xi/\delta = 0.29$, curve 3 – $\xi/\delta = 0.39$, curve 4 – $\xi/\delta = 0.48$, curve 5 – $\xi/\delta = 1.86$ and curve 6 – $\xi/\delta = 3.67$. Phase spectra (Fig. 12b) were plotted for pairs of sensors divided by distance:

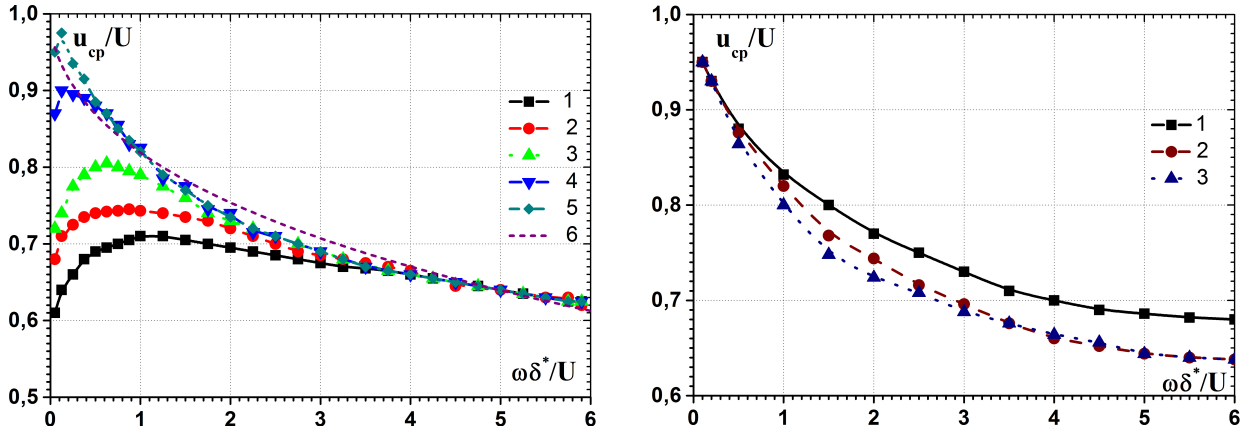

Fig. 13. Convective velocities of the coherent vortex structures inside the turbulent boundary layer above the flexible cylinder for $\delta/R = 2.5$:
1 — $\xi/\delta = 0.19$, *2* — $\xi/\delta = 0.39$, *3* — $\xi/\delta = 0.85$,
4 — $\xi/\delta = 6.27$, *5* — $\xi/\delta = 10.43$, *6* — the envelope curve

Fig. 14. Convective velocities of the coherent vortex structures inside the turbulent boundary layer above the flexible cylinder for $\delta/R = (3 \dots 7)$:
1 — $\delta/R = 7$; *2* — $\delta/R = 4$; *3* — $\delta/R = 3$

curve *1* – $\xi/\delta = 0.19$, curve *2* – $\xi/\delta = 0.29$, and curve *3* – $\xi/\delta = 0.39$. The phase of the cross-spectrum monotonically changed with increasing frequency in the low-frequency region. The inclination of the phase was decreased with increasing of the frequency and decreasing of the sensor separation. The direction of phase change made it possible to determine the direction of transfer of coherent vortex structures, in this case, in the direction of motion, and also to determine the convective velocity of vortex structures in the form $u_{cp} = \xi/[2\pi\Delta\Theta(\xi,\omega)/\Delta\omega]$.

Subsequent plots represent the dependences of the dimensionless phase convective velocities of coherent vortex structures generating wall pressure fluctuations on the streamlined surface of a flexible cylinder, from the frequency for various separations between sensors and transverse curvatures of extended cylinders. Curve *1* in Fig. 13 was obtained for separation $\xi/\delta = 0.19$, curve *2* – $\xi/\delta = 0.39$, curve *3* – $\xi/\delta = 0.85$, curve *4* – $\xi/\delta = 6.27$, curve *3* – $\xi/\delta = 10.43$ and curve *6* is the envelope line, which was obtained in research [62, 82] and calculated according to the dependence $u_{cp} = U\exp[-0.2(\omega\delta^*/U)^{1/2}]$. Results were measured on the flexible cylinder with transverse curvature $\delta/R \approx 2.5$ and Reynolds numbers $\mathrm{Re}_X = 4 \cdot 10^7$ and $\mathrm{Re}_R = 7 \cdot 10^4$. The research results show that the phase convective velocity increases with increasing frequency in the low-frequency region, reaches a maximum, and decreases monotonically in the high-frequency region. A similar behavior of the phase convective velocity was first discovered in a paper [67] on smooth and rough flat surfaces. Such behavior was manifested to a lesser extent when the separation between the sensors was increased, and a decrease of the convective velocity at low frequencies for the separation $\xi^* \geq 100$ was not observed. The convective velocity of coherent vortex structures decreased monotonically with increasing frequency. Thus, large-scale vortex structures of the boundary layer convected downstream at a velocity that was close to the towing velocity of the cylinder [30, 34]. Small-scale vortex structures that formed the wall region of the boundary

layer and generated high-frequency pressure fluctuations had convective velocity $u_{cp} \approx 0.6U$.

Fig. 14 shows the dependence of the change in the phase convective velocities of the coherent vortex structures under the influence of the transverse curvature of streamlined flexible cylinders. Curve *1* was obtained for the cylinder with a diameter of 16 mm and the transverse curvature of $\delta/R = 7$, curve *2* – 29 mm and $\delta/R = 4$, curve *3* – 44 mm and $\delta/R = 3$. The research results showed that above the flexible cylinder of the small diameter, which had the transverse curvature $\delta/R = 7$, the convective velocity of the coherent vortex structures was higher than above cylinders that had the small transverse curvature. Since the velocity profile of the boundary layer was more filled on the cylinder, which had the smaller diameter [62, 80, 83], the phase convective velocity of the coherent vortex structures of a given scale will be higher.

4. CONCLUSIONS

Research results showed that the transformation of the flow energy into the energy of the wall pressure fluctuation field has a limiting value, which corresponds to an acoustic-hydrodynamic coefficient (ratio of root-mean-square values of the wall pressure fluctuations to the dynamic pressure) of the order of 0.01 on a hydraulically smooth streamlined surface beneath a turbulent boundary layer with a zero-pressure gradient.

The space-time correlation of the wall pressure fluctuations along the generatrix of a flexible extended cylinder is decreased with increasing distance between the observation points, and the maximum cross-correlation values are observed for a longer delay time. Consequently, small-scale vortices are degenerated with increasing distance along the surface of the cylinder, and large-scale vortices remain correlated structures. It was found that on the flexible cylinder, the attenuation rate of the maximum values of the cross-correlation coefficients was higher than on the plate but lower than on the rigid cylinder.

The “lifetime” of pressure forming large-scale vortex structures, which generated low-frequency wall pressure fluctuations, was 4 to 5 times higher than the “lifetime” of small-scale low-velocity vortices that generated high-frequency fluctuations of the pressure field on the cylindrical surface of the flexible longitudinal streamlined cylinder.

The group convective velocity of transfer of coherent vortex structures that are generated over the surface of a flexible cylinder is higher than over the surface of a rigid cylinder and over the surface of a smooth and rough plate. The group and local convective velocities of large-scale vortex structures are higher than those of small-scale eddies.

The coherence of the pressure fluctuation field along the generatrix of the flexible extended cylinder decreased with an increase in the separation between the sensors and the frequency, since small-scale vortex structures lost their individuality faster than large-scale coherent vortex structures. The phase of the cross-spectrum monotonically changed with increasing frequency in the low-frequency region. The inclination of the phase spectrum dependence decreased with increasing frequency and decreasing sensor separation. The slope of phase curves decreased with decreasing convective velocity.

The convective velocity phase increases with increasing frequency in the low-frequency region, reaches a maximum, and decreases monotonically in the high-frequency region. The convective velocity of the coherent vortex structures above the flexible cylinder of the small diameter was higher than above cylinders that had a small transverse curvature. Small-

scale vortices, which generate high-frequency pressure fluctuations, degenerate faster and are convected more slowly than large-scale coherent vortex structures that form the outer region of the boundary layer.

REFERENCES

[1] A. Amron, R. R. Hidayat, M. D. Nur Meinita, and M. Trenggono, "Underwater noise of traditional fishing boats in Cilacap waters, Indonesia," *Heliyon*, vol. 7, no. 11, pp. e08 364 (1–7), 2021. DOI: https://doi.org/10.1016/j.heliyon.2021.e08364

[2] M. J. Jurado, M. Ripepe, C. Lopez, A. Ricciardi, M. J. Blanco, and G. Lacanna, "Underwater records of submarine volcanic activity: El Hierro (Canary Islands 2011–2012) eruption," *Journal of Volcanology and Geothermal Research*, vol. 408, pp. 107 097 (1–10), Dec. 2020. DOI: https://doi.org/10.1016/j.jvolgeores.2020.107097

[3] S. Li, D. E. Rival, and X. Wu, "Sound source and pseudo-sound in the near field of a circular cylinder in subsonic conditions," *Journal of Fluid Mechanics*, vol. 919, pp. A43 (1–33), 2021. DOI: https://doi.org/10.1017/jfm.2021.404

[4] T. Pillay, H. C. Cawthra, and A. T. Lombard, "Integration of machine learning using hydroacoustic techniques and sediment sampling to refine substrate description in the Western Cape, South Africa," *Marine Geology*, vol. 440, pp. 106 599 (1–16), 2021. DOI: https://doi.org/10.1016/j.margeo.2021.106599

[5] S. A. Villar, A. Madirolas, A. G. Cabreira, A. Rozenfeld, and G. G. Acosta, "ECOPAMPA: A new tool for automatic fish schools detection and assessment from echo data," *Heliyon*, vol. 7, no. 1, pp. e05 906 (1–10), 2021. DOI: https://doi.org/10.1016/j.heliyon.2021.e05906

[6] J. E. Ffowks Williams, "Hydrodynamic noise," *Annual Review of Fluid Mechanics*, vol. 1, no. 1, pp. 197–222, 1969. DOI: https://doi.org/10.1146/annurev.fl.01.010169.001213

[7] M. Wang, J. B. Freund, and S. K. Lele, "Computational prediction of flow-generated sound," *Annual Review of Fluid Mechanics*, vol. 38, no. 1, pp. 483–512, 2006. DOI: https://doi.org/10.1146/annurev.fluid.38.050304.092036

[8] M. Mancinelli, T. Pagliaroli, A. Di Marco, R. Camussi, and T. Castelain, "Wavelet decomposition of hydrodynamic and acoustic pressures in the near field of the jet," *Journal of Fluid Mechanics*, vol. 813, pp. 716–749, 2017. DOI: https://doi.org/10.1017/jfm.2016.869

[9] J. Song, D. Jung, J. S. Kim, and J. Lee, "Experimental evaluation of pseudo-sound in a parametric array," *The Journal of the Acoustical Society of America*, vol. 150, no. 5, pp. 3787–3796, 2021. DOI: https://doi.org/10.1121/10.0007279

[10] A. K. M. Fazle Hussain, "Coherent structures and turbulence," *Journal of Fluid Mechanics*, vol. 173, pp. 303–356, 1986. DOI: https://doi.org/10.1017/s0022112086001192

[11] J. Jiménez, "Coherent structures in wall-bounded turbulence," *Journal of Fluid Mechanics*, vol. 842, pp. P1 (1–100), 2018. DOI: https://doi.org/10.1017/jfm.2018.144

[12] J. R. Ristorcelli, "A pseudo-sound constitutive relationship for the dilatational covariances in compressible turbulence," *Journal of Fluid Mechanics*, vol. 347, pp. 37–70, 1997. DOI: https://doi.org/10.1017/s0022112097006083

[13] A. V. Smol'yakov, "Calculation of the spectra of pseudosound wall-pressure fluctuations in turbulent boundary layers," *Acoustical Physics*, vol. 46, no. 3, pp. 342–347, 2000. DOI: https://doi.org/10.1134/1.29890

[14] M. Felli, S. Grizzi, and M. Falchi, "A novel approach for the isolation of the sound and pseudo-sound contributions from near-field pressure fluctuation measurements: analysis of the hydroacoustic and hydrodynamic perturbation in a propeller-rudder system," *Experiments in Fluids*, vol. 55, no. 1, pp. 1651 (1–17), 2013. DOI: https://doi.org/10.1007/s00348-013-1651-y

[15] K. N. Volkov, V. N. Emel'yanov, and A. G. Karpenko, "Pseudosound pressure oscillations caused by the interaction of a fluid flow with the obstacle in the form of a circular cylinder in a pipe," *Journal of Engineering Physics and Thermophysics*, vol. 95, no. 1, pp. 80–89, 2022. DOI: https://doi.org/10.1007/s10891-022-02455-5

[16] W. W. Willmarth, "Pressure fluctuations beneath turbulent boundary layers," *Annual Review of Fluid Mechanics*, vol. 7, no. 1, pp. 13–36, 1975. DOI: https://doi.org/10.1146/annurev.fl.07.010175.000305

[17] A. V. Smol'yakov, *Noise of turbulent flows*. Saint Petersburg: Krylov Shipbuilding Research Institute, 2005.

[18] A. K. Banerjee and S. K. Singh, "Parametric investigation of spatio-temporal variability of submerged body hydrodynamics," *Applied Ocean Research*, vol. 123, pp. 103 152 (1–17), 2022. DOI: https://doi.org/10.1016/j.apor.2022.103152

[19] R. L. Panton and J. H. Linebarger, "Wall pressure spectra calculations for equilibrium boundary layers," *Journal of Fluid Mechanics*, vol. 65, no. 2, pp. 261–287, 1974. DOI: https://doi.org/10.1017/s0022112074001388

[20] G. A. Gerolymos, D. Sénéchal, and I. Vallet, "Wall effects on pressure fluctuations in turbulent channel flow," *Journal of Fluid Mechanics*, vol. 720, pp. 15–65, 2013. DOI: https://doi.org/10.1017/jfm.2012.633

[21] M. Slama, C. Leblond, and P. Sagaut, "A Kriging-based elliptic extended anisotropic model for the turbulent boundary layer wall pressure spectrum," *Journal of Fluid Mechanics*, vol. 840, pp. 25–55, 2018. DOI: https://doi.org/10.1017/jfm.2017.810

[22] G. Grasso, P. Jaiswal, H. Wu, S. Moreau, and M. Roger, "Analytical models of the wall-pressure spectrum under a turbulent boundary layer with adverse pressure gradient," *Journal of Fluid Mechanics*, vol. 877, pp. 1007–1062, 2019. DOI: https://doi.org/10.1017/jfm.2019.616

[23] K. C. Kim and R. J. Adrian, "Very large-scale motion in the outer layer," *Physics of Fluids*, vol. 11, no. 2, pp. 417–422, 1999. DOI: https://doi.org/10.1063/1.869889

[24] H. Abe, H. Kawamura, and H. Choi, "Very large-scale structures and their effects on the wall shear-stress fluctuations in a turbulent channel flow up to $\mathrm{Re}_\tau = 640$," *Journal of Fluids Engineering*, vol. 126, no. 5, pp. 835–843, 2004. DOI: https://doi.org/10.1115/1.1789528

[25] N. Hutchins and I. Marusic, "Evidence of very long meandering features in the logarithmic region of turbulent boundary layers," *Journal of Fluid Mechanics*, vol. 579, pp. 1–28, 2007. DOI: https://doi.org/10.1017/s0022112006003946

[26] R. Mathis, N. Hutchins, and I. Marusic, "Large-scale amplitude modulation of the small-scale structures in turbulent boundary layers," *Journal of Fluid Mechanics*, vol. 628, pp. 311–337, 2009. DOI: https://doi.org/10.1017/s0022112009006946

[27] B. Ganapathisubramani, N. Hutchins, J. P. Monty, D. Chung, and I. Marusic, "Amplitude and frequency modulation in wall turbulence," *Journal of Fluid Mechanics*, vol. 712, pp. 61–91, 2012. DOI: https://doi.org/10.1017/jfm.2012.398

[28] M. Cho, Y. Hwang, and H. Choi, "Scale interactions and spectral energy transfer in turbulent channel flow," *Journal of Fluid Mechanics*, vol. 854, pp. 474–504, 2018. DOI: https://doi.org/10.1017/jfm.2018.643

[29] J. Chen, M. Zhu, R. Zhang, and J. Li, "Numerical simulation and flow noise computation during transient launching process of torpedo in deep-sea simulator," *Applied Ocean Research*, vol. 121, pp. 103 095 (1–15), 2022. DOI: https://doi.org/10.1016/j.apor.2022.103095

[30] J. C. Del Álamo, J. Jiménez, P. Zandonade, and R. D. Moser, "Scaling of the energy spectra of turbulent channels," *Journal of Fluid Mechanics*, vol. 500, pp. 135–144, 2004. DOI: https://doi.org/10.1017/s002211200300733x

[31] S. Hoyas, M. Oberlack, F. Alcántara-Ávila, S. V. Kraheberger, and J. Laux, "Wall turbulence at high friction Reynolds numbers," *Physical Review Fluids*, vol. 7, no. 1, pp. 014 602 (1–10), 2022. DOI: https://doi.org/10.1103/physrevfluids.7.014602

[32] T. M. Farabee and M. J. Casarella, "Spectral features of wall pressure fluctuations beneath turbulent boundary layers," *Physics of Fluids A: Fluid Dynamics*, vol. 3, no. 10, pp. 2410–2420, 1991. DOI: https://doi.org/10.1063/1.858179

[33] T. Chen, T. Liu, Z.-Q. Dong, L.-P. Wang, and S. Chen, "Near-wall flow structures and related surface quantities in wall-bounded turbulence," *Physics of Fluids*, vol. 33, no. 6, pp. 065 116 (1–33), 2021. DOI: https://doi.org/10.1063/5.0051649

[34] G. P. Vinogradnyi, V. A. Voskoboinik, V. T. Grinchenko, and A. P. Makarenkov, "Spectral and correlation characteristics of the turbulent boundary layer on an extended flexible cylinder," *Fluid Dynamics*, vol. 24, no. 5, pp. 695–700, 1990. DOI: https://doi.org/10.1007/bf01051721

[35] M. K. Bull, "Wall-pressure fluctuations beneath turbulent boundary layers: some reflections on forty years of research," *Journal of Sound and Vibration*, vol. 190, no. 3, pp. 299–315, 1996. DOI: https://doi.org/10.1006/jsvi.1996.0066

[36] V. A. Voskoboinick, V. T. Grinchenko, and A. P. Makarenkov, "Correlation characteristics of a wall pressure fluctuation field in a turbulent boundary layer induced by a longitudinal flow along a flexible extended cylinder," *International Journal of Fluid Mechanics Research*, vol. 30, no. 6, pp. 644–650, 2003. DOI: https://doi.org/10.1615/interjfluidmechres.v30.i6.70

[37] J. S. Bendat and A. G. Piersol, *Random data: Analysis and measurement procedures*. New York: John Wiley & Sons, 2011.

[38] R. H. Kraichnan, "Pressure fluctuations in turbulent flow over a flat plate," *The Journal of the Acoustical Society of America*, vol. 28, no. 3, pp. 378–390, 1956. DOI: https://doi.org/10.1121/1.1908336

[39] W. Blake, *Mechanics of flow-induced sound and vibration*. New York: Academic Press, 1986, vol. 1: General concepts and elementary sources.

[40] G. M. Corcos, "Resolution of pressure in turbulence," *The Journal of the Acoustical Society of America*, vol. 35, no. 2, pp. 192–199, 1963. DOI: https://doi.org/10.1121/1.1918431

[41] D. M. Chase, "Modeling the wavevector-frequency spectrum of turbulent boundary layer wall pressure," *Journal of Sound and Vibration*, vol. 70, no. 1, pp. 29–67, 1980. DOI: https://doi.org/10.1016/0022-460x(80)90553-2

[42] M. Goody, "Empirical spectral model of surface pressure fluctuations," *AIAA Journal*, vol. 42, no. 9, pp. 1788–1794, 2004. DOI: https://doi.org/10.2514/1.9433

[43] A. V. Smol'yakov, "A new model for the cross spectrum and wavenumber-frequency spectrum of turbulent pressure fluctuations in a boundary layer," *Acoustical Physics*, vol. 52, no. 3, pp. 331–337, 2006. DOI: https://doi.org/10.1134/s1063771006030146

[44] N. Hu, "Empirical model of wall pressure spectra in adverse pressure gradients," *AIAA Journal*, vol. 56, no. 9, pp. 3491–3506, 2018. DOI: https://doi.org/10.2514/1.j056666

[45] S. Lee, "Empirical wall-pressure spectral modeling for zero and adverse pressure gradient flows," *AIAA Journal*, vol. 56, no. 5, pp. 1818–1829, 2018. DOI: https://doi.org/10.2514/1.j056528

[46] K. Ritos, D. Drikakis, and I. W. Kokkinakis, "Wall-pressure spectra models for supersonic and hypersonic turbulent boundary layers," *Journal of Sound and Vibration*, vol. 443, pp. 90–108, 2019. DOI: https://doi.org/10.1016/j.jsv.2018.11.001

[47] J. Dominique, J. Christophe, C. Schram, and R. D. Sandberg, "Inferring empirical wall pressure spectral models with Gene Expression Programming," *Journal of Sound and Vibration*, vol. 506, pp. 116 162 (1–18), 2021. DOI: https://doi.org/10.1016/j.jsv.2021.116162

[48] W. R. Graham, "A comparison of models for the wavenumber–frequency spectrum of turbulent boundary layer pressures," *Journal of Sound and Vibration*, vol. 206, no. 4, pp. 541–565, 1997. DOI: https://doi.org/10.1006/jsvi.1997.1114

[49] Y. F. Hwang, W. K. Bonness, and S. A. Hambric, "Comparison of semi-empirical models for turbulent boundary layer wall pressure spectra," *Journal of Sound and Vibration*, vol. 319, no. 1-2, pp. 199–217, 2009. DOI: https://doi.org/10.1016/j.jsv.2008.06.002

[50] B. Yang and Z. Yang, "On the wavenumber–frequency spectrum of the wall pressure fluctuations in turbulent channel flow," *Journal of Fluid Mechanics*, vol. 937, pp. A39 (1–27), 2022. DOI: https://doi.org/10.1017/jfm.2022.137

[51] O. M. Phillips, "On the aerodynamic surface sound from a plane turbulent boundary layer," *Proceedings of the Royal Society of London. Series A.*, vol. 234, no. 1198, pp. 327–335, 1956. DOI: https://doi.org/10.1098/rspa.1956.0037

[52] M. S. Howe, "A note on the Kraichnan–Phillips theorem," *Journal of Fluid Mechanics*, vol. 234, pp. 443–448, 1992. DOI: https://doi.org/10.1017/s0022112092000855

[53] P. Bradshaw, "'Inactive' motion and pressure fluctuations in turbulent boundary layers," *Journal of Fluid Mechanics*, vol. 30, no. 2, pp. 241–258, 1967. DOI: https://doi.org/10.1017/s0022112067001417

[54] B. Gibeau and S. Ghaemi, "Low- and mid-frequency wall-pressure sources in a turbulent boundary layer," *Journal of Fluid Mechanics*, vol. 918, pp. A18 (1–45), 2021. DOI: https://doi.org/10.1017/jfm.2021.339

[55] V. A. Voskoboinick, "Space-time characteristics of coherent structures, velocity and pressure fields into the dimpled vortex generators," Doctor Thesis, Institute of Hydromechanics of NASU, Kyiv, 2013.

[56] V. A. Voskoboinick, V. N. Turick, O. A. Voskoboinyk, A. V. Voskoboinick, and I. A. Tereshchenko, *Influence of the deep spherical dimple on the pressure field under the turbulent boundary layer*. Cham: Springer International Publishing, 2018, vol. 754, pp. 23–32. DOI: https://doi.org/10.1007/978-3-319-91008-6

[57] S. Shubham, R. D. Sandberg, S. Moreau, and H. Wu, "Surface pressure spectrum variation with Mach number on a CD airfoil," *Journal of Sound and Vibration*, vol. 526, pp. 116 762 (1–15), 2022. DOI: https://doi.org/10.1016/j.jsv.2022.116762

[58] V. A. Voskoboinik, A. A. Voskoboinik, V. N. Turik, and A. V. Voskoboinik, "Space and time characteristics of the velocity and pressure fields of the fluid flow inside a hemispherical dimple generator of vortices," *Journal of Engineering Physics and Thermophysics*, vol. 93, no. 5, pp. 1205–1220, 2020. DOI: https://doi.org/10.1007/s10891-020-02223-3

[59] V. A. Voskoboinick and A. P. Makarenkov, "Spectral characteristics of the pseudosonic component of hydrodynamical noise in a longitudinal flow around a flexible cylinder,"

International Journal of Fluid Mechanics Research, vol. 31, no. 1, pp. 87–100, 2004. DOI: https://doi.org/10.1615/interjfluidmechres.v31.i1.70

[60] V. A. Voskoboinick, V. T. Grinchenko, and A. P. Makarenkov, "Pseudo-sound behind an obstacle on a cylinder in axial flow," *International Journal of Fluid Mechanics Research*, vol. 32, no. 4, pp. 488–510, 2005. DOI: https://doi.org/10.1615/interjfluidmechres.v32.i4.60

[61] G. P. Vinogradnyi, M. V. Kanarskii, and A. P. Makarenkov, "A device for the dynamic calibration of pressure sensors," USSR patent 1 029 021, 1983.

[62] V. A. Voskoboinick, "Wall-pressure fluctuations of turbulent boundary layer on streamlined flexible extended cylinder," Cand. Thesis, Institute of Hydromechanics of Acad. Sci. Ukraine, Kyiv, 1993.

[63] A. Meshkinzar and A. M. Al-Jumaily, "Vibration and acoustic radiation characteristics of cylindrical piezoelectric transducers with circumferential steps," *Journal of Sound and Vibration*, vol. 511, pp. 116 346 (1–16), 2021. DOI: https://doi.org/10.1016/j.jsv.2021.116346

[64] M. K. Bull, "Wall-pressure fluctuations associated with subsonic turbulent boundary layer flow," *Journal of Fluid Mechanics*, vol. 28, no. 4, pp. 719–754, 1967. DOI: https://doi.org/10.1017/s0022112067002411

[65] G. Schewe, "On the structure and resolution of wall-pressure fluctuations associated with turbulent boundary-layer flow," *Journal of Fluid Mechanics*, vol. 134, pp. 311–328, 1983. DOI: https://doi.org/10.1017/s0022112083003389

[66] T. Langeheineken and A. Dinkelacker, "Wand druckschwankungen einer ausgebildeten, turbulenten Rohrströmung," in *Fortschritte der Akustik – DAGA'78*. Berlin: VDE-Verlag, 1978, pp. 391–394.

[67] W. K. Blake, "Turbulent boundary-layer wall-pressure fluctuations on smooth and rough walls," *Journal of Fluid Mechanics*, vol. 44, no. 4, pp. 637–660, 1970. DOI: https://doi.org/10.1017/s0022112070002069

[68] M. K. Bull and A. S. W. Thomas, "High frequency wall-pressure fluctuations in turbulent boundary layers," *Physics of Fluids*, vol. 19, no. 4, pp. 597–599, 1976. DOI: https://doi.org/10.1063/1.861496

[69] J. Andreopoulos and J. H. Agui, "Wall-vorticity flux dynamics in a two-dimensional turbulent boundary layer," *Journal of Fluid Mechanics*, vol. 309, pp. 45–84, 1996. DOI: https://doi.org/10.1017/s0022112096001553

[70] E. S. Winkel, B. R. Elbing, S. L. Ceccio, M. Perlin, and D. R. Dowling, "High-Reynolds-number turbulent-boundary-layer wall pressure fluctuations with skin-friction reduction by air injection," *The Journal of the Acoustical Society of America*, vol. 123, no. 5, pp. 2522–2530, 2008. DOI: https://doi.org/10.1121/1.2902169

[71] N. D. Varano, "Fluid dynamics and surface pressure fluctuations of turbulent boundary layers over sparse roughness," Ph. D. Thesis, Virginia Polytechnic Institute, Blacksburg, VA, 2010.

[72] M. C. Goody and R. L. Simpson, "Surface pressure fluctuations beneath two- and three-dimensional turbulent boundary layers," *AIAA Journal*, vol. 38, no. 10, pp. 1822–1831, 2000. DOI: https://doi.org/10.2514/2.863

[73] S. P. Gravante, A. M. Naguib, C. E. Wark, and H. M. Nagib, "Characterization of the pressure fluctuations under a fully developed turbulent boundary layer," *AIAA Journal*, vol. 36, no. 10, pp. 1808–1816, 1998. DOI: https://doi.org/10.2514/2.296

[74] Y. Tsuji, J. H. M. Fransson, P. H. Alfredsson, and A. V. Johansson, "Pressure statistics and their scaling in high-Reynolds-number turbulent boundary layers," *Journal of Fluid Mechanics*, vol. 585, pp. 1–40, Aug. 2007. DOI: https://doi.org/10.1017/s0022112007006076

[75] R. M. Lueptow, "Transducer resolution and the turbulent wall pressure spectrum," *The Journal of the Acoustical Society of America*, vol. 97, no. 1, pp. 370–378, 1995. DOI: https://doi.org/10.1121/1.412322

[76] W. L. Keith, D. A. Hurdis, and B. M. Abraham, "A comparison of turbulent boundary layer wall-pressure spectra," *Journal of Fluids Engineering*, vol. 114, no. 3, pp. 338–347, 1992. DOI: https://doi.org/10.1115/1.2910035

[77] D. Gatti, A. Stroh, B. Frohnapfel, and R. Örlü, "Spatial resolution issues in rough wall turbulence," *Experiments in Fluids*, vol. 63, no. 3, pp. 63 (1–6), 2022. DOI: https://doi.org/10.1007/s00348-022-03412-x

[78] W. W. Willmarth, R. E. Winkel, L. K. Sharma, and T. J. Bogar, "Axially symmetric turbulent boundary layers on cylinders: mean velocity profiles and wall pressure fluctuations," *Journal of Fluid Mechanics*, vol. 76, no. 1, pp. 35–64, 1976. DOI: https://doi.org/10.1017/s002211207600311x

[79] W. W. Willmarth and C. E. Wooldridge, "Measurements of the fluctuating pressure at the wall beneath a thick turbulent boundary layer," *Journal of Fluid Mechanics*, vol. 14, no. 2, pp. 187–210, 1962. DOI: https://doi.org/10.1017/s0022112062001160

[80] W. W. Willmarth and C. S. Yang, "Wall-pressure fluctuations beneath turbulent boundary layers on a flat plate and a cylinder," *Journal of Fluid Mechanics*, vol. 41, no. 1, pp. 47–80, 1970. DOI: https://doi.org/10.1017/s0022112070000526

[81] N. Hu, "Coherence of wall pressure fluctuations in zero and adverse pressure gradients," *Journal of Sound and Vibration*, vol. 511, pp. 116 316 (1–27), 2021. DOI: https://doi.org/10.1016/j.jsv.2021.116316

[82] V. A. Voskoboinick, V. T. Grinchenko, and A. P. Makarenkov, "The velocities of convection of coherent vortex structures in a turbulent boundary layer on the cylinder," *Acoustic Bulletin*, vol. 3, no. 4, pp. 21–29, 2000.

[83] G. N. V. Rao and N. R. Keshavan, "Axisymmetric turbulent boundary layers in zero pressure-gradient flows," *Journal of Applied Mechanics*, vol. 39, no. 1, pp. 25–32, 1972. DOI: https://doi.org/10.1115/1.3422623

ЛІТЕРАТУРА

[1] Underwater noise of traditional fishing boats in Cilacap waters, Indonesia / Amron A., Hidayat R. R., Nur Meinita M. D., and Trenggono M. // Heliyon. — 2021. — Vol. 7, no. 11. — P. e08364 (1–7).

[2] Underwater records of submarine volcanic activity: El Hierro (Canary Islands 2011–2012) eruption / Jurado M. J., Ripepe M., Lopez C., Ricciardi A., Blanco M. J., and Lacanna G. // Journal of Volcanology and Geothermal Research. — 2020. — Dec. — Vol. 408. — P. 107097 (1–10).

[3] Li S., Rival D. E., Wu X. Sound source and pseudo-sound in the near field of a circular cylinder in subsonic conditions // Journal of Fluid Mechanics. — 2021. — Vol. 919. — P. A43 (1–33).

[4] Pillay T., Cawthra H. C., Lombard A. T. Integration of machine learning using hydroacoustic techniques and sediment sampling to refine substrate description in the Western Cape, South Africa // Marine Geology. — 2021. — Vol. 440. — P. 106599 (1–16).

[5] ECOPAMPA: A new tool for automatic fish schools detection and assessment from echo data / Villar S. A., Madirolas A., Cabreira A. G., Rozenfeld A., and Acosta G. G. // Heliyon. — 2021. — Vol. 7, no. 1. — P. e05906 (1–10).

[6] Ffowks Williams J. E. Hydrodynamic noise // Annual Review of Fluid Mechanics. — 1969. — Vol. 1, no. 1. — P. 197–222.

[7] Wang M., Freund J. B., Lele S. K. Computational prediction of flow-generated sound // Annual Review of Fluid Mechanics. — 2006. — Vol. 38, no. 1. — P. 483–512.

[8] Wavelet decomposition of hydrodynamic and acoustic pressures in the near field of the jet / Mancinelli M., Pagliaroli T., Di Marco A., Camussi R., and Castelain T. // Journal of Fluid Mechanics. — 2017. — Vol. 813. — P. 716–749.

[9] Experimental evaluation of pseudo-sound in a parametric array / Song J., Jung D., Kim J. S., and Lee J. // The Journal of the Acoustical Society of America. — 2021. — Vol. 150, no. 5. — P. 3787–3796.

[10] Fazle Hussain A. K. M. Coherent structures and turbulence // Journal of Fluid Mechanics. — 1986. — Vol. 173. — P. 303–356.

[11] Jiménez J. Coherent structures in wall-bounded turbulence // Journal of Fluid Mechanics. — 2018. — Vol. 842. — P. P1 (1–100).

[12] Ristorcelli J. R. A pseudo-sound constitutive relationship for the dilatational covariances in compressible turbulence // Journal of Fluid Mechanics. — 1997. — Vol. 347. — P. 37–70.

[13] Смольяков А. В. Вычисление спектров псевдозвуковых флуктуаций пристеночных давлений в турбулентных пограничных слоях // Акустический журнал. — 2000. — Т. 46, № 3. — С. 342–347.

[14] Felli M., Grizzi S., Falchi M. A novel approach for the isolation of the sound and pseudo-sound contributions from near-field pressure fluctuation measurements: analysis of the hydroacoustic and hydrodynamic perturbation in a propeller-rudder system // Experiments in Fluids. — 2013. — Vol. 55, no. 1. — P. 1651 (1–17).

[15] Волков К. Н., Емельянов В. Н., Карпенко А. Г. Псевдозвуковые пульсации давления, обусловленные взаимодействием потока жидкости в трубе с препятствием в виде круглого цилиндра // Инженерно-физический журнал. — 2022. — Т. 95, № 1. — С. 81–90.

[16] Willmarth W. W. Pressure fluctuations beneath turbulent boundary layers // Annual Review of Fluid Mechanics. — 1975. — Vol. 7, no. 1. — P. 13–36.

[17] Смольяков А. В. Шум турбулентных потоков. — Санкт-Петербург : ЦНИИ им. акад. А. Н. Крылова, 2005. — 311 с.

[18] Banerjee A. K., Singh S. K. Parametric investigation of spatio-temporal variability of submerged body hydrodynamics // Applied Ocean Research. — 2022. — Vol. 123. — P. 103152 (1–17).

[19] Panton R. L., Linebarger J. H. Wall pressure spectra calculations for equilibrium boundary layers // Journal of Fluid Mechanics. — 1974. — Vol. 65, no. 2. — P. 261–287.

[20] Gerolymos G. A., Sénéchal D., Vallet I. Wall effects on pressure fluctuations in turbulent channel flow // Journal of Fluid Mechanics. — 2013. — Vol. 720. — P. 15–65.

[21] Slama M., Leblond C., Sagaut P. A Kriging-based elliptic extended anisotropic model for the turbulent boundary layer wall pressure spectrum // Journal of Fluid Mechanics. — 2018. — Vol. 840. — P. 25–55.

[22] Analytical models of the wall-pressure spectrum under a turbulent boundary layer with adverse pressure gradient / Grasso G., Jaiswal P., Wu H., Moreau S., and Roger M. // Journal of Fluid Mechanics. — 2019. — Vol. 877. — P. 1007–1062.

[23] Kim K. C., Adrian R. J. Very large-scale motion in the outer layer // Physics of Fluids. — 1999. — Vol. 11, no. 2. — P. 417–422.

[24] Abe H., Kawamura H., Choi H. Very large-scale structures and their effects on the wall shear-stress fluctuations in a turbulent channel flow up to $\mathrm{Re}_\tau = 640$ // Journal of Fluids Engineering. — 2004. — Vol. 126, no. 5. — P. 835–843.

[25] Hutchins N., Marusic I. Evidence of very long meandering features in the logarithmic region of turbulent boundary layers // Journal of Fluid Mechanics. — 2007. — Vol. 579. — P. 1–28.

[26] Mathis R., Hutchins N., Marusic I. Large-scale amplitude modulation of the small-scale structures in turbulent boundary layers // Journal of Fluid Mechanics. — 2009. — Vol. 628. — P. 311–337.

[27] Amplitude and frequency modulation in wall turbulence / Ganapathisubramani B., Hutchins N., Monty J. P., Chung D., and Marusic I. // Journal of Fluid Mechanics. — 2012. — Vol. 712. — P. 61–91.

[28] Cho M., Hwang Y., Choi H. Scale interactions and spectral energy transfer in turbulent channel flow // Journal of Fluid Mechanics. — 2018. — Vol. 854. — P. 474–504.

[29] Numerical simulation and flow noise computation during transient launching process of torpedo in deep-sea simulator / Chen J., Zhu M., Zhang R., and Li J. // Applied Ocean Research. — 2022. — Vol. 121. — P. 103095 (1–15).

[30] Scaling of the energy spectra of turbulent channels / Del Álamo J. C., Jiménez J., Zandonade P., and Moser R. D. // Journal of Fluid Mechanics. — 2004. — Vol. 500. — P. 135–144.

[31] Wall turbulence at high friction Reynolds numbers / Hoyas S., Oberlack M., Alcántara-Ávila F., Kraheberger S. V., and Laux J. // Physical Review Fluids. — 2022. — Vol. 7, no. 1. — P. 014602 (1–10).

[32] Farabee T. M., Casarella M. J. Spectral features of wall pressure fluctuations beneath turbulent boundary layers // Physics of Fluids A: Fluid Dynamics. — 1991. — Vol. 3, no. 10. — P. 2410–2420.

[33] Near-wall flow structures and related surface quantities in wall-bounded turbulence / Chen T., Liu T., Dong Z.-Q., Wang L.-P., and Chen S. // Physics of Fluids. — 2021. — Vol. 33, no. 6. — P. 065116 (1–33).

[34] Spectral and correlation characteristics of the turbulent boundary layer on an extended flexible cylinder / Vinogradnyi G. P., Voskoboinik V. A., Grinchenko V. T., and Makarenkov A. P. // Fluid Dynamics. — 1990. — Vol. 24, no. 5. — P. 695–700.

[35] Bull M. K. Wall-pressure fluctuations beneath turbulent boundary layers: some reflections on forty years of research // Journal of Sound and Vibration. — 1996. — Vol. 190, no. 3. — P. 299–315.

[36] Voskoboinick V. A., Grinchenko V. T., Makarenkov A. P. Correlation characteristics of a wall pressure fluctuation field in a turbulent boundary layer induced by a longitudinal flow along a flexible extended cylinder // International Journal of Fluid Mechanics Research. — 2003. — Vol. 30, no. 6. — P. 644–650.

[37] Bendat J. S., Piersol A. G. Random data: Analysis and measurement procedures. — New York : John Wiley & Sons, 2011. — 640 p.

[38] Kraichnan R. H. Pressure fluctuations in turbulent flow over a flat plate // The Journal of the Acoustical Society of America. — 1956. — Vol. 28, no. 3. — P. 378–390.

[39] Blake W. Mechanics of flow-induced sound and vibration. — New York : Academic Press, 1986. — Vol. 1: General concepts and elementary sources. — 502 p.

[40] Corcos G. M. Resolution of pressure in turbulence // The Journal of the Acoustical Society of America. — 1963. — Vol. 35, no. 2. — P. 192–199.

[41] Chase D. M. Modeling the wavevector-frequency spectrum of turbulent boundary layer wall pressure // Journal of Sound and Vibration. — 1980. — Vol. 70, no. 1. — P. 29–67.

[42] Goody M. Empirical spectral model of surface pressure fluctuations // AIAA Journal. — 2004. — Vol. 42, no. 9. — P. 1788–1794.

[43] Смольяков А. В. Новая модель взаимного и частотно-волнового спектров турбулентных пульсаций давления в пограничном слое // Акустический журнал. — 2006. — Т. 52, № 3. — С. 331–337.

[44] Hu N. Empirical model of wall pressure spectra in adverse pressure gradients // AIAA Journal. — 2018. — Vol. 56, no. 9. — P. 3491–3506.

[45] Lee S. Empirical wall-pressure spectral modeling for zero and adverse pressure gradient flows // AIAA Journal. — 2018. — Vol. 56, no. 5. — P. 1818–1829.

[46] Ritos K., Drikakis D., Kokkinakis I. W. Wall-pressure spectra models for supersonic and hypersonic turbulent boundary layers // Journal of Sound and Vibration. — 2019. — Vol. 443. — P. 90–108.

[47] Inferring empirical wall pressure spectral models with Gene Expression Programming / Dominique J., Christophe J., Schram C., and Sandberg R. D. // Journal of Sound and Vibration. — 2021. — Vol. 506. — P. 116162 (1–18).

[48] Graham W. R. A comparison of models for the wavenumber–frequency spectrum of turbulent boundary layer pressures // Journal of Sound and Vibration. — 1997. — Vol. 206, no. 4. — P. 541–565.

[49] Hwang Y. F., Bonness W. K., Hambric S. A. Comparison of semi-empirical models for turbulent boundary layer wall pressure spectra // Journal of Sound and Vibration. — 2009. — Vol. 319, no. 1-2. — P. 199–217.

[50] Yang B., Yang Z. On the wavenumber–frequency spectrum of the wall pressure fluctuations in turbulent channel flow // Journal of Fluid Mechanics. — 2022. — Vol. 937. — P. A39 (1–27).

[51] Phillips O. M. On the aerodynamic surface sound from a plane turbulent boundary layer // Proceedings of the Royal Society of London. Series A. — 1956. — Vol. 234, no. 1198. — P. 327–335.

[52] Howe M. S. A note on the Kraichnan–Phillips theorem // Journal of Fluid Mechanics. — 1992. — Vol. 234. — P. 443–448.

[53] Bradshaw P. 'Inactive' motion and pressure fluctuations in turbulent boundary layers // Journal of Fluid Mechanics. — 1967. — Vol. 30, no. 2. — P. 241–258.

[54] Gibeau B., Ghaemi S. Low- and mid-frequency wall-pressure sources in a turbulent boundary layer // Journal of Fluid Mechanics. — 2021. — Vol. 918. — P. A18 (1–45).

[55] Воскобійник В. А. Просторово-часові характеристики когерентних структур, полів швидкості та тиску у лункових генераторах вихорів : дис. ... докт. наук ; Інститут гідромеханіки НАН України. — Київ, 2013. — 422 с.

[56] Influence of the deep spherical dimple on the pressure field under the turbulent boundary layer / Voskoboinick V. A., Turick V. N., Voskoboinyk O. A., Voskoboinick A. V., and Tereshchenko I. A. // Advances in Computer Science for Engineering and Education. — Cham : Springer International Publishing, 2018. — Vol. 754. — P. 23–32.

[57] Surface pressure spectrum variation with Mach number on a CD airfoil / Shubham S., Sandberg R. D., Moreau S., and Wu H. // Journal of Sound and Vibration. — 2022. — Vol. 526. — P. 116762 (1–15).

[58] Пространственно-временные характеристики поля скорости и давления внутри полусферического луночного генератора вихрей / Воскобойник В. А., Воскобойник А. А., Турик В. Н. и Воскобойник А. В. // Инженерно-физический журнал. — 2020. — Т. 93, № 5. — С. 1248–1264.

[59] Voskoboinick V. A., Makarenkov A. P. Spectral characteristics of the pseudosonic component of hydrodynamical noise in a longitudinal flow around a flexible cylinder // International Journal of Fluid Mechanics Research. — 2004. — Vol. 31, no. 1. — P. 87–100.

[60] Voskoboinick V. A., Grinchenko V. T., Makarenkov A. P. Pseudo-sound behind an obstacle on a cylinder in axial flow // International Journal of Fluid Mechanics Research. — 2005. — Vol. 32, no. 4. — P. 488–510.

[61] Устройство для динамической тарировки датчиков давления : патент СССР 1029021 / Виноградный Г. П., Канарский М. В., Макаренков А. П. // Бюллетень изобретателя. — 1983. — № 5.

[62] Воскобойник В. А. Пульсации пристеночного давления турбулентного пограничного слоя, образованного при обтекании гибкого протяженного цилиндра : дис. ... канд. наук ; Институт гидромеханики АН Украины. — Киев, 1993.

[63] Meshkinzar A., Al-Jumaily A. M. Vibration and acoustic radiation characteristics of cylindrical piezoelectric transducers with circumferential steps // Journal of Sound and Vibration. — 2021. — Vol. 511. — P. 116346 (1–16).

[64] Bull M. K. Wall-pressure fluctuations associated with subsonic turbulent boundary layer flow // Journal of Fluid Mechanics. — 1967. — Vol. 28, no. 4. — P. 719–754.

[65] Schewe G. On the structure and resolution of wall-pressure fluctuations associated with turbulent boundary-layer flow // Journal of Fluid Mechanics. — 1983. — Vol. 134. — P. 311–328.

[66] Langeheineken T., Dinkelacker A. Wand druckschwankungen einer ausgebildeten, turbulenten Rohrströmung // Fortschritte der Akustik – DAGA'78. — Berlin : VDE-Verlag. — 1978. — S. 391–394.

[67] Blake W. K. Turbulent boundary-layer wall-pressure fluctuations on smooth and rough walls // Journal of Fluid Mechanics. — 1970. — Vol. 44, no. 4. — P. 637–660.

[68] Bull M. K., Thomas A. S. W. High frequency wall-pressure fluctuations in turbulent boundary layers // Physics of Fluids. — 1976. — Vol. 19, no. 4. — P. 597–599.

[69] Andreopoulos J., Agui J. H. Wall-vorticity flux dynamics in a two-dimensional turbulent boundary layer // Journal of Fluid Mechanics. — 1996. — Vol. 309. — P. 45–84.

[70] High-Reynolds-number turbulent-boundary-layer wall pressure fluctuations with skin-friction reduction by air injection / Winkel E. S., Elbing B. R., Ceccio S. L., Perlin M., and Dowling D. R. // The Journal of the Acoustical Society of America. — 2008. — Vol. 123, no. 5. — P. 2522–2530.

[71] Varano N. D. Fluid dynamics and surface pressure fluctuations of turbulent boundary layers over sparse roughness : Ph. D. Thesis ; Virginia Polytechnic Institute. — Blacksburg, VA, 2010.

[72] Goody M. C., Simpson R. L. Surface pressure fluctuations beneath two- and three-dimensional turbulent boundary layers // AIAA Journal. — 2000. — Vol. 38, no. 10. — P. 1822–1831.

[73] Characterization of the pressure fluctuations under a fully developed turbulent boundary layer / Gravante S. P., Naguib A. M., Wark C. E., and Nagib H. M. // AIAA Journal. — 1998. — Vol. 36, no. 10. — P. 1808–1816.

[74] Pressure statistics and their scaling in high-Reynolds-number turbulent boundary layers / Tsuji Y., Fransson J. H. M., Alfredsson P. H., and Johansson A. V. // Journal of Fluid Mechanics. — 2007. — Aug. — Vol. 585. — P. 1–40.

[75] Lueptow R. M. Transducer resolution and the turbulent wall pressure spectrum // The Journal of the Acoustical Society of America. — 1995. — Vol. 97, no. 1. — P. 370–378.

[76] Keith W. L., Hurdis D. A., Abraham B. M. A comparison of turbulent boundary layer wall-pressure spectra // Journal of Fluids Engineering. — 1992. — Vol. 114, no. 3. — P. 338–347.

[77] Spatial resolution issues in rough wall turbulence / Gatti D., Stroh A., Frohnapfel B., and Örlü R. // Experiments in Fluids. — 2022. — Vol. 63, no. 3. — P. 63 (1–6).

[78] Axially symmetric turbulent boundary layers on cylinders: mean velocity profiles and wall pressure fluctuations / Willmarth W. W., Winkel R. E., Sharma L. K., and Bogar T. J. // Journal of Fluid Mechanics. — 1976. — Vol. 76, no. 1. — P. 35–64.

[79] Willmarth W. W., Wooldridge C. E. Measurements of the fluctuating pressure at the wall beneath a thick turbulent boundary layer // Journal of Fluid Mechanics. — 1962. — Vol. 14, no. 2. — P. 187–210.

[80] Willmarth W. W., Yang C. S. Wall-pressure fluctuations beneath turbulent boundary layers on a flat plate and a cylinder // Journal of Fluid Mechanics. — 1970. — Vol. 41, no. 1. — P. 47–80.

[81] Hu N. Coherence of wall pressure fluctuations in zero and adverse pressure gradients // Journal of Sound and Vibration. — 2021. — Vol. 511. — P. 116316 (1–27).

[82] Воскобойник В. А., Гринченко В. Т., Макаренков А. П. Скорости переноса когерентных вихревых структур втурбулентном пограничном слое на цилиндре // Акустичний вісник. — 2000. — Т. 3, № 4. — С. 21–29.

[83] Rao G. N. V., Keshavan N. R. Axisymmetric turbulent boundary layers in zero pressure-gradient flows // Journal of Applied Mechanics. — 1972. — Vol. 39, no. 1. — P. 25–32.

В. А. Воскобійник, В. Т. Грінченко,
О. А. Воскобійник, А. В. Воскобійник

Просторово-часові характеристики пристінкових пульсацій тиску на поверхні гнучкого протяжного циліндра

Генерація гідродинамічного або аеродинамічного шуму є добре відомою проблемою для транспортних засобів та конструкцій, що рухаються у водному або повітряному середовищах. Тому прогнозування та керування властивостями турбулентних гідродинамічних псевдоакустичних джерел має велике значення. У цій статті представлено результати експериментального дослідження взаємних кореляцій та взаємних спектрів пристінкових пульсацій тиску на поверхні поздовжньо обтічного гнучкого циліндра. Показано, що ступінь перетворення енергії потоку в енергію поля коливань тиску на стінці обмежений певним порогом. Його значення відповідає відношенню середньоквадратичних пульсацій тиску на стінці до динамічного тиску порядку 0.01 на гідравлічно гладкій обтічній поверхні під турбулентним примежовим шаром з нульовим градієнтом тиску. Просторово-часова кореляція пульсацій тиску на стінці вздовж твірної гнучкого протяжного циліндра зменшується зі збільшенням відстані між точками спостереження, а максимальні значення взаємної кореляції спостерігаються для більших часів затримки. Конвекція когерентних

вихрових структур над обтічною поверхнею циліндра призводить до збільшення рівнів когерентності поля пристінкових пульсацій тиску. Більш того, спостерігаються зміни у фазовому спектрі, який представлено похилими кривими. Їхній нахил зменшується зі збільшенням конвективної швидкості. Швидкість виродження максимальних значень коефіцієнта просторово-часової кореляції в широкому діапазоні частот на гнучкому циліндрі вища, ніж на пластині. Дрібномасштабні вихри, що генерують високочастотні коливання тиску, вироджуються швидше та переносяться повільніше, ніж великомасштабні когерентні вихрові структури із зовнішньої області примежового шару. Отримані результати будуть корисними для розробників буксируваних лінійних приймальних гідроакустичних ґраток.

КЛЮЧОВІ СЛОВА: просторово-часові характеристики, пристінкові пульсації тиску, гнучкий циліндр, взаємна кореляція, когерентність, фазовий спектр